

Dynamics and fluctuations during MBE on vicinal surfaces. II. Nonlinear analysis

O. Pierre-Louis* and C. Misbah

*Laboratoire de Spectrométrie Physique, Université Joseph Fourier, CNRS, Grenoble I, Boîte Postale 87,
Saint-Martin d'Hères, 38402 Cedex, France*

(Received 2 September 1997)

This paper is the natural next step beyond the linear regime presented in the preceding paper. By concentrating on the situation close to the step morphological instability threshold, we derive nonlinear evolution equations for interacting steps on a vicinal train. This treatment is coherent in that it retains only relevant nonlinearities close enough to the threshold. Our analysis provides the expression of the coefficients in terms of thermodynamic and transport coefficients. Numerical analysis of these equations reveals spatially and temporally disordered patterns. We give a criterion specifying the region where step roughness is due to both stochastic effects (associated with various sources of noise) and deterministic ones (stemming from deterministic spatiotemporal chaos). Outside this region, the roughness is dominated by either stochastic or deterministic effects. Starting from the discrete version (this is taken to mean that each step is described as an entity) of step dynamics (that is to say, each step is separately described by an evolution equation), we derive a coarse-grained evolution equation for the surface. This results in an anisotropic Kuramoto-Sivashinsky equation including propagative effects. Numerical analysis reveals situations where the original surface undergoes a secondary instability leading ultimately to a rough pattern. The surface looks as if two-dimensional nucleation were allowed. Implication and outlooks are discussed. [S0163-1829(98)06127-X]

I. INTRODUCTION

This paper considers the nonlinear evolution of steps on a vicinal surface submitted to molecular beam epitaxy in a regime where growth is achieved by step flow, that is to say, two-dimensional (2D) island nucleation is prohibited. The model rests on that of Burton, Cabrera, and Frank supplemented with step noninstantaneous kinetics, elastic interaction, and fluctuations. Starting from this model (generally combining basic principles, namely, conservation and kinetic laws), we shall derive continuum evolution equations for steps dynamics, from which the surface evolution equation can be extracted. Unlike phenomenological studies, this work provides a general basis for the derivation of evolution equations, where the form, magnitude of nonlinearities, and expression of coefficients are extracted in a systematic manner. It also shows that phenomenological studies can lack several terms. A typical example is that this treatment allows a derivation of the Kardar-Parisi-Zhang¹ (KPZ) equation from microscopic consideration, an equation that holds for an isolated step and when allowance is made of finite desorption. For a train of steps we obtain equations for nonlinear interacting lines.

We have presented in the preceding paper (hereafter referred to as I) the model equations and studied the equilibrium and nonequilibrium features in the linear regime. We have seen that as the deposition flux is increased, we reach a critical value, above which the steps become morphologically unstable. This implies that nonlinear effects become important. At arbitrary distance from the threshold dynamics is highly nonlinear. However, by concentrating on the situation close to the threshold, we can extract from the nonlocal and nonlinear equations only the part that is relevant in this regime. A weakly nonlinear analysis becomes legitimate. On the other hand, because of translational symmetries, the most

dangerous modes are the long-wavelength ones. This will imply that close to the threshold the dynamics is local in both space and time. We shall derive in a coherent way nonlinear evolution equations for steps dynamics. We consider the general case where the steps are not synchronized, though it will emerge that the in-phase motion is the most dominant one. As a simple introduction we shall first concentrate on the case of an isolated step. This will allow us to rederive from an integral equation the evolution equation derived by Bena *et al.*² This will serve as a preparation for the derivation of the evolution equations in a train. This is a problem where each step is interacting with its neighbors via both the diffusion field and the elastic one. We shall then analyze the equations numerically. We find generically disordered patterns. We specify both static and dynamical structure factors. For the spatial behavior, we find that the value of the exponent of the structure factor as a function of the wave number is the same as the one of an isolated step on a large scale. On short scales, rather strong correlations are found. The dynamical structure factor reveals a typical frequency associated with propagative effects. Indeed, phase shifts between two steps evolve in a propagative manner. This is even recognized in the linear dispersion relation, where the eigenvalue has an imaginary part when the phase shift is nonzero. Moreover, localized fluctuations appearing on a step are always advected upward, that is, they propagate in the direction opposite the global train motion.

The next step is devoted to the continuum limit starting from the discrete version derived from the integral equations. That is, from the step evolution equations we derive a coarse-grained equation for the surface evolution. This results in an anisotropic Kuramoto-Sivashinsky equation with propagative terms. It emerges from our study that the vicinal surface may suffer a secondary instability, leading ultimately to a rough surface. The structure is very reminiscent of that

appearing on a nominal surface and is implied by the Ehrlich-Schwöbel effect. A similar behavior has been found by Rost *et al.*³ in a model equation having a completely different form and introduced in the context of growth in the absence of desorption.

The scheme of this paper is as follows. In Sec. II we deal with the limit of an isolated step. In Sec. III, we write the evolution equations for the train. In Sec. IV we present the main lines of the derivations. Section V deals with the exploitation of the nonlinear results of step dynamics. Section VI is devoted to the continuum limit. The conclusion and outlooks is the subject of Sec. VII. Details and some lengthy expressions are relegated to the Appendixes.

II. ISOLATED STEP

A. Integral formulation

Before tackling the problem of a train of steps on a vicinal surface, which is the main purpose of this paper, we shall first depict the dynamics of an isolated step.² The derivation presented here differs significantly from that given in the original paper,² by direct use of an integral formulation. Thus we find it worthwhile to devote a brief discussion to this point.

It is possible to derive a closed integro-differential equation for the meander of an isolated step (i.e., without referring to the adatom concentration) when the model is one sided ($d_- \rightarrow \infty$). For the sake of simplicity, we restrict our analysis to the instantaneous attachment case $d_+ = 0$. Using the relation (22) in I, the concentration in front of the step u_+ is related to the meander ζ by

$$\begin{aligned} \frac{u_+}{2} &= \tau \int dt' \int dx' \left[1 + (\partial \zeta' / \partial x')^2 \right]^{1/2} \\ &\times D \left(u'_+ \frac{\partial G}{\partial n'} - G \frac{\partial u'_+}{\partial n'} \right) - (V + \zeta') G u'_+ \\ &+ \Omega \tau \int dt' \int dx' \int dz' (f' - \nabla \cdot \mathbf{q}') \\ &\times G(x - x', \zeta - z', t - t'), \end{aligned} \quad (1)$$

where $G = G(x - x', \zeta(x, t) - \zeta(x', t'), t - t')$ and $\dot{\zeta} = \partial \zeta / \partial t$. The prime indicates that the arguments are x' and t' [for example, $\zeta = \zeta(x, t)$ and $\zeta' = \zeta(x', t')$]. The concentration u_+ and its normal derivative obey the relations [see Eqs. (24) and (14) in I]

$$u_+ = -\Omega c_{eq}^0 \sigma + \Gamma \kappa - \Omega \eta_+, \quad (2)$$

$$\frac{\partial u_+}{\partial n} = \frac{1}{D} \left(\frac{V + \dot{\zeta}}{\sqrt{1 + \left(\frac{\partial \zeta}{\partial x} \right)^2}} + \Omega \mathbf{n} \cdot \mathbf{q}_+ \right). \quad (3)$$

Inserting these expressions into Eq. (1), we find

$$\begin{aligned} &\int dt' \int dx' \frac{Y(\Delta t)}{4\pi D \Delta t} e^{-\Delta t/\tau - (\Delta x^2 + \Delta \zeta^2)/4D\Delta t} \\ &\times \left\{ \frac{1}{2\Delta t} \left(-\frac{\partial \zeta'}{\partial x'} \Delta x + \Delta \zeta \right) [-\Omega c_{eq}^0 \sigma + \Gamma \kappa' - \Omega \eta'_+] \right. \\ &- (V + \zeta') - \Omega \left(-\frac{\partial \zeta'}{\partial x'} q'_x + q'_z \right) \\ &\left. + \zeta' (\Omega c_{eq}^0 \sigma - \Gamma \kappa' + \Omega \eta'_+) \right\} \\ &+ \Omega \int dt' \int dx' \int dz' \frac{Y(\Delta t)}{4\pi D \Delta t} \\ &\times e^{-\Delta t/\tau - [\Delta x^2 + (z' - \zeta)^2]/4D\Delta t} \{ f' - \nabla \cdot \mathbf{q}' \} \\ &= \frac{1}{2} (-\Omega c_{eq}^0 \sigma + \Gamma \kappa - \Omega \eta_+), \end{aligned} \quad (4)$$

where we have defined $\Delta x = x - x'$, $\Delta t = t - t'$, and $\Delta \zeta = \zeta - \zeta'$. This result is a closed integro-differential equation for the isolated step, which exhibits explicitly the nonlinear and nonlocal features of the step dynamics. The only reference to what happens on the terraces is due to the cumulated effect of the conserved and nonconserved fluctuations of the adatom concentration. The deterministic part of this equation depends only on the step configuration and of its history.

This type of formulation offers possibilities in numerical treatment⁴ of step dynamics. Here we intend to extract analytically the relevant nonlinearities by means of a multiple scale analysis close to the instability threshold.

B. Linear analysis and spatiotemporal scales

Our calculation is based on an expansion with respect to a small parameter that measures the departure from the instability threshold

$$\epsilon = \frac{\sigma - \sigma_{BZ}}{\sigma_{BZ}}, \quad (5)$$

where σ_{BZ} is the value of the supersaturation at the instability threshold [see Eq. (68) in I]. The spatiotemporal active scales are fixed by the linear analysis and behave as

$$x \sim \epsilon^{\vartheta_x}, \quad t \sim \epsilon^{\vartheta_t}, \quad (6)$$

where ϑ_x and ϑ_t are exponents to be determined below.

To leading order, Eq. (4) provides the mean velocity $V = \sigma c_{eq}^0 \sqrt{D/\tau}$ for a straight step. This velocity is proportional to the departure from equilibrium through the supersaturation σ . Equation (4) is expanded to first order in ζ [see Eq. (A1)]. In Fourier space, we find an equation for the Fourier transform of the meander $\zeta_{\omega k} = \int dx \int dt \zeta(x, t) e^{-i\omega t - ikx}$, which is written as

$$\chi_{\omega k}^{-1} \zeta_{\omega k} = \beta_{\omega k}. \quad (7)$$

$\chi_{\omega k}$ is the susceptibility of the step meander

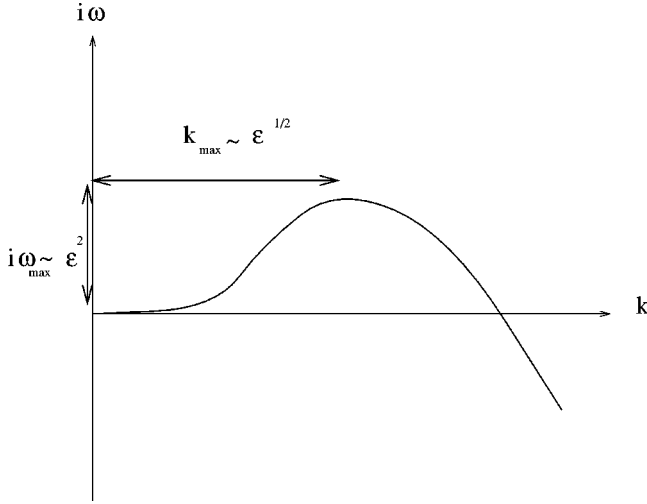


FIG. 1. Dispersion relation for an isolated step. The most unstable mode has a wave number $k = k_{max} \sim \epsilon^{1/2}$ and its linear growth rate is $i\omega = i\omega_{max} \sim \epsilon^2$.

$$\chi_{\omega k}^{-1} = i\omega + \left(\frac{D}{\tau}\right)^{1/2} \Gamma k^2 \sqrt{k^2 x_s^2 + i\omega\tau + 1} + \frac{\Omega c_{eq}^0}{\tau} \times \sigma(1 - \sqrt{k^2 x_s^2 + i\omega\tau + 1}). \quad (8)$$

The step is subject to a noise β resulting from a combination of the Langevin forces introduced in the model. β obeys the following correlations law at equilibrium:

$$\langle |\beta_{\omega k}|^2 \rangle = \frac{\Omega^2 c_{eq}}{\text{Re}(\Lambda_{\omega k})} [|\Lambda_{\omega k}|^2 + \text{Re}(\Lambda_{\omega k}^2)] \left(\frac{D}{\tau}\right)^{1/2}, \quad (9)$$

where $\Lambda_{\omega k} = (k^2 + i\omega/D + 1/x_s^2)^{1/2}$. The additional contributions coming from the departure from equilibrium are found to be negligible.

In the quasistatic and long-wavelength limits ($i\omega \ll Dk^2 \ll 1/\tau$), the dispersion relation in Fourier space is of the form

$$i\omega(k) \approx \epsilon a k^2 - b k^4. \quad (10)$$

If $a > 0$ (or $\sigma > 2\Gamma/\Omega c_{eq}^0 x_s$ [see Eq. (67) in I]), a straight step is unstable. The most unstable mode is $k_{max} = \epsilon^{1/2} \sqrt{a/2b}$. The growth rate of this mode is $i\omega_{max} = \epsilon^2 a^2/4b$ (see Fig. 1). These relations provide the order of magnitude of the scales associated with active modes. This defines the characteristic spatiotemporal scales of the instability. In real space we have $x \sim 2\pi/k_{max} \sim \epsilon^{-1/2}$ and $t \sim 2\pi/\omega_{max} \sim \epsilon^{-2}$, which lead to

$$\vartheta_x = -\frac{1}{2}, \quad \vartheta_t = -2. \quad (11)$$

C. Relevant nonlinearity

An inspection of Eq. (4) shows that the first nonlinearity is provided by the term

$$I = -V \int dt' \int dx' \frac{Y(\Delta t)}{4\pi D \Delta t} e^{-\Delta t/\tau - (\Delta x^2 + \Delta \zeta^2)/4D \Delta t}. \quad (12)$$

Since the dynamics are local, a Taylor expansion $\Delta \zeta^2 \sim (\Delta x)^2 (\partial \zeta / \partial x)^2 + \mathcal{L}$ (where \mathcal{L} denotes higher-order terms) is allowed, so that

$$I = -V \int dt' \int dx' \frac{Y(\Delta t)}{4\pi D \Delta t} e^{-\Delta t/\tau - \Delta x^2 [1 + (\partial \zeta / \partial x)^2]/4D \Delta t} \approx \frac{V}{2} \left(\frac{\tau}{D}\right)^{1/2} \left[-1 + \frac{1}{2} \left(\frac{\partial \zeta}{\partial x}\right)^2 \right]. \quad (13)$$

Inserting this term into Eq. (10) expressed in real space and using Eq. (7) for the noise term, we find the noisy Kuramoto-Sivashinsky equation

$$\frac{\partial \zeta}{\partial t} = -\Omega c_{eq}^0 \frac{D}{2} (\sigma - \sigma_{BZ}) \frac{\partial^2 \zeta}{\partial x^2} - \Omega c_{eq}^0 \frac{D^2 \tau}{4} \left(\sigma + \frac{\sigma_{BZ}}{2} \right) \frac{\partial^4 \zeta}{\partial x^4} + \frac{V}{2} \left(\frac{\partial \zeta}{\partial x}\right)^2 + \beta, \quad (14)$$

where the Langevin force β obeys [see Eq. (9)]

$$\langle |\beta_{\omega k}|^2 \rangle = 2\Omega^2 c_{eq}^0 \left(\frac{D}{\tau}\right)^{1/2} \quad (15)$$

in the quasistatic and long-wavelength limits.

Note that below the instability threshold ($\sigma < \sigma_{BZ}$), the fourth derivative can be ignored in Eq. (14) (since there is no need for a cutoff) and we recover the KPZ equation.

The form of the nonlinearity was expected since the translational invariance of the step properties with respect to the step position forbids nonlinearities that include ζ but allows its derivatives $\partial^n \zeta / \partial x^n$. The first nonlinearity (which is compatible with $x \rightarrow -x$ symmetry) that satisfies this condition is $(\partial \zeta / \partial x)^2$. This nonlinearity appears in a wide variety of out of equilibrium systems, such as laminar flame propagation⁵ and solidification at large undercooling,⁶ and its genericity has been shown.⁷

Note that the prefactor of the nonlinearity $V/2 = \sigma c_{eq}^0 \sqrt{D/\tau}/2$ is proportional to the departure from equilibrium via σ . This indicates that this nonlinear term is absent at equilibrium. An important property of this term is that it cannot be obtained from an energetic picture via the relation $\partial \zeta / \partial t = \delta \mathcal{H} / \delta \zeta$, where \mathcal{H} is an energy functional: The out-of-equilibrium dynamics of the meander does not possess a Lyapunov functional. Defining the dimensionless variables $\tilde{x} = (8/3)^{1/2} x/x_s$, $\tilde{t} = (8D\Omega c_{eq}^0 \sigma_{BZ}/3x_s^2)t$, and $h = \zeta/x_s$, Eq. (14) takes the form

$$\frac{\partial h}{\partial \tilde{t}} = -\nu \frac{\partial^2 h}{\partial \tilde{x}^2} - \mu \frac{\partial^4 h}{\partial \tilde{x}^4} + \frac{\lambda}{2} \left(\frac{\partial h}{\partial \tilde{x}}\right)^2 + \theta, \quad (16)$$

with the noise correlation

$$\langle \theta(\tilde{x}, h) \theta(\tilde{x}', h') \rangle = \theta_0 \delta(\tilde{x} - \tilde{x}') \delta(\tilde{t} - \tilde{t}'), \quad (17)$$

where we have defined the parameters

$$\lambda = \sigma / \sigma_{BZ}, \quad (18)$$

$$\nu = (\sigma - \sigma_{BZ}) / 2\sigma_{BZ},$$

$$\mu = 2(1 + \sigma/2\sigma_{BZ})/3,$$

$$\theta_0 = (3/8)^{1/2} k_B T / \gamma x_s.$$

D. Competition between stochasticity and determinism

We have already given a brief account of this question.⁸ Here we provide a simple discussion on the competition between noise and the deterministic instability. Since the steps are one-dimensional entities, they are subject to large statistical fluctuations. When driven out of equilibrium (e.g., during growth), the steps are also subject to a morphological instability. In this section we develop an analysis of the competition between these two phenomena.⁸

Let us rescale Eq. (16) using the transformations

$$\tilde{t} = \alpha_t^{-1} T, \quad \tilde{x} = \alpha_x^{-1} X, \quad (19)$$

$$h(\tilde{t}, \tilde{x}) = \alpha_h H(X, T).$$

The result is an evolution equation expressed in terms of X , T , and H ,

$$\begin{aligned} \frac{\partial H}{\partial T} = & -\alpha_x^2 \alpha_t^{-1} \nu \frac{\partial^2 H}{\partial X^2} - \alpha_x^4 \alpha_t^{-1} \mu \frac{\partial^4 H}{\partial X^4} \\ & + \alpha_h \alpha_x^2 \alpha_t^{-1} \frac{\lambda}{2} \left(\frac{\partial H}{\partial X} \right)^2 + \Theta. \end{aligned} \quad (20)$$

We define the Langevin force $\Theta = \alpha_h^{-1} \alpha_t^{-1} \theta$, whose correlation reads

$$\langle \Theta(X, T) \Theta(X', T') \rangle = \theta_0 \alpha_h^{-2} \alpha_x \alpha_t^{-1} \delta(X - X') \delta(T - T'). \quad (21)$$

First, we choose the prefactors of the linear terms of Eq. (20) to be one (actually, any factor of that order will provide the same results). That is to say, we assume that only linear behavior fixes the spatial and temporal scales. This yields

$$\alpha_x = \left(\frac{|\nu|}{\mu} \right)^{1/2}, \quad \alpha_t = \frac{\nu^2}{\mu}. \quad (22)$$

In reality nonlinear terms will intervene as soon as the instability develops and fix the amplitude of modulation. As is visible in Eq. (20), the amplitude scale enters the nonlinear term. Because the noise is additive in Eq. (20) its correlation is inversely proportional to the amplitude squared. This is expressed by Eq. (21), where α_h^{-2} enters. Therefore the amplitude of the modulation is determined either by the nonlinear deterministic part or by the noise amplitude. These two conditions are obtained by setting either the prefactor of the nonlinear term or the amplitude of the noise to order one. This entails two different scalings for h ,

$$\alpha_h = \frac{|\nu|}{\lambda}, \quad \alpha_h = \theta_0^{1/2} \frac{\mu^{1/4}}{|\nu|^{3/4}}. \quad (23)$$

The region where both statistical fluctuations and deterministic chaos are present is the region where these two scalings are of the same order of magnitude. This leads to

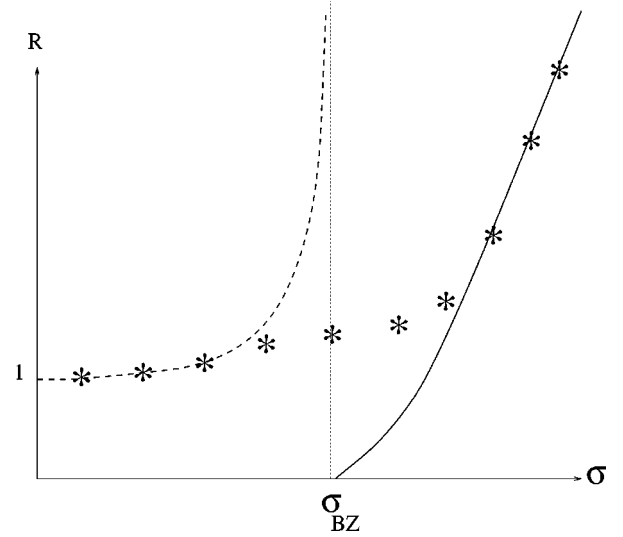


FIG. 2. Roughness of an isolated step as a function of the supersaturation. The dashed lines indicate the linear theory. The solid line indicates the nonlinear deterministic theory. The asterisks are the results of numerical simulations.

$$\theta_0 \frac{\mu^{1/2} \lambda^2}{|\nu|^{7/2}} \sim 1. \quad (24)$$

Since the region of this competition is around the threshold where nonlinearities become relevant, we can set $\lambda \approx 1$ and $\mu \approx 1$. This leads to a Ginzburg-Landau-like criterion, expressing the width of the region where competition between statistical noise and deterministic chaos is strong. This is readily given by

$$|\nu| \sim \theta_0^{2/7}. \quad (25)$$

If $\nu < 0$ and $|\nu| \gg \theta_0^{2/7}$ then the meander is governed by statistical fluctuations. If $\nu > 0$ and $|\nu| \ll \theta_0^{2/7}$, the roughness is of deterministic origin. In that case the dynamics of the meander is chaotic in space and time since it is governed by the deterministic Kuramoto-Sivashinsky equation. The short-length-scale modes play the role of an effective noise (spatiotemporal chaos produces its own noise). In between, when $|\nu| < \theta_0^{2/7}$, both noise and deterministic chaos are present. Note that the determination of the region where stochastic and deterministic effects compete (25) did not require the knowledge of the spectrum behavior ($\langle |h_k|^2 \rangle \sim 1/k^2$). The explicit form of the roughness (given in Ref. 8) did, however, need that information (see Fig. 2). As for the study of the roughness, we refer to Ref. 8.

III. TRAIN OF STEPS

A. Spatiotemporal scales

Let us now consider the case of a train of steps. We still consider the quasistatic limit. We first determine the spatiotemporal scalings from an inspection of the linear dispersion relation. Here, besides the time t and the lateral space variable x , we have an additional discrete degree of freedom, which is the index m of the steps. We also have to determine its scaling behavior. To do so, we consider its Fourier con-

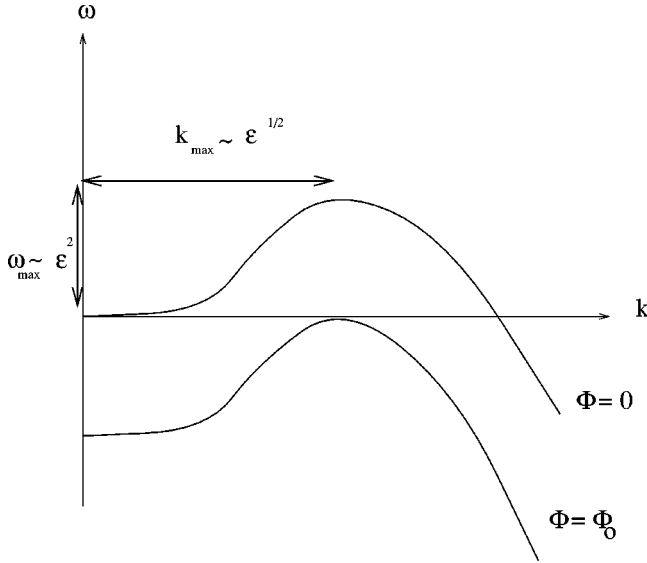


FIG. 3. Dispersion relation of a train of steps. The most unstable mode has a wave number $k = k_{\max} \sim \epsilon^{1/2}$ and its linear growth rate is $i\omega = i\omega_{\max} \sim \epsilon^2$. The phase cutoff is $\Phi_0 \sim \epsilon$.

jugate variable Φ . The most unstable mode is the in-phase mode ($\Phi = 0$). Its linear dispersion relation is similar to Eq. (10):

$$i\omega(k, \Phi = 0) = \epsilon ak^2 - bk^4. \quad (26)$$

The real part of $i\omega$ concerns the growth or decay rate of the small perturbations. The imaginary part of $i\omega$ depicts the propagation of these perturbations. Here the imaginary part of $i\omega$ is equal to zero and $i\omega$ is real. The dispersion relation (26) leads to the same exponents as in the case with an isolated step for x and t : $\partial_x = -1/2$ and $\partial_t = -2$. Now we consider modes such that $\Phi \neq 0$ and $\Phi \ll 1$. Then $i\omega$ has an imaginary part. Since we are interested in the stability of the train of steps, we first restrict ourselves to the real part of the dispersion relation. Their dispersion relation has the form (see Fig. 3)

$$\text{Re}[i\omega(k, \Phi)] = \epsilon ak^2 - bk^4 - c\Phi^2. \quad (27)$$

We now determine the scaling of Φ . The modes Φ that contribute to the instability are those for which there exists a value k^* such that $\text{Re}[i\omega(k^*, \Phi)] > 0$. This condition is fulfilled for $\Phi < \Phi_0 = \epsilon a/2\sqrt{bc}$. Moreover, to be relevant, the $c\Phi^2$ term in Eq. (27) must be at least of the same order as the other terms, which scale like ϵ^2 , so that $\Phi \geq \epsilon$. We therefore conclude that $\Phi \sim \epsilon$. In real space this means that $\zeta_m - \zeta_{m+1}$ is of the same order as $\epsilon \zeta_m$. We define the exponent ϑ_m via the relation $\Phi \sim \epsilon^{-\vartheta_m}$. Here we have $\vartheta_m = -1$.

The imaginary part of the dispersion relation is deduced from the expression of the susceptibility [Eq. (B16) in I]. This leads to

$$\text{Im}[i\omega(k, \Phi)] = \sin(\Phi)g(k^2). \quad (28)$$

Since $\sin(\Phi) = 0$ when $\Phi = 0$ or $\Phi = \pi$, there is no propagative effect for the in-phase and the out-of-phase modes. The imaginary part of the dispersion relation does not affect the

scaling of the space and time variables. As a consequence of these scalings, the leading order and the subdominant term of Eq. (28) are written as

$$\text{Im}[i\omega(k, \Phi)] \approx \Phi g_0 + \Phi k^2 g_2. \quad (29)$$

g_0 and g_2 are calculated from a large-scale limit ($k \sim \epsilon^{1/2}$ and $\Phi \sim \epsilon$, with $\epsilon \rightarrow 0$) of g . Their expressions are given in Appendix B. Note that $\Phi k^2 g_2 \sim \epsilon^2$. This term is therefore of the same order as the real part of the dispersion relation. This corresponds to time scales $t \sim \epsilon^{-2}$.

The other term is $\Phi g_0 \sim \epsilon$. It introduces a shorter time scale associated with the propagative effects $t \sim \epsilon^{-1}$. The positive sign of g_0 indicates that the perturbations are advected backward (in the $-z$ direction).

B. Multiple scale analysis

Let us first give a general discussion based on scaling and symmetry to derive the form of the relevant nonlinear equations. In Sec. IV we outline how these equations are extracted from the microscopic model.

The translational invariance of the whole train of steps implies that ζ can appear in the equation of motion in two different ways: first, in terms of its derivatives with respect to x ($\partial\zeta/\partial x$, $\partial^2\zeta/\partial x^2$...), and second, in terms of finite difference expressions with respect to the step index [$\zeta_m(x, t) - \zeta_{m-1}(x, t)$, $\zeta_{m+1}(x, t) + \zeta_{m-1}(x, t) - 2\zeta_m(x, t)$, ...]. Mixtures are also possible [$\partial\zeta_m(x, t)/\partial x - \partial\zeta_{m-1}(x, t)/\partial x$, ...]. Since we must preserve the symmetry $x \rightarrow -x$, some terms are forbidden [$\partial\zeta_m(x, t)/\partial x$, ...]. This allows us to determine the scaling of all the possible nonlinearities that are quadratic in ζ ,

$$\begin{aligned} (\zeta_{m+1} - \zeta_m)^2 &\sim \epsilon^2 \zeta^2, \\ \left(\frac{\partial\zeta}{\partial x}\right)^2 &\sim \epsilon \zeta^2, \end{aligned} \quad (30)$$

$$(\zeta_{m+1} - \zeta_m) \frac{\partial^2\zeta}{\partial x^2} \sim \epsilon^2 \zeta^2,$$

etc. It is easy to check that the dominant term is $(\partial\zeta/\partial x)^2$. Since the linear propagative terms (corresponding to the imaginary part of the linear dispersion relation) do not contribute to the scaling properties of the instability itself (but do for propagation; see below), we shall first omit them. The nonlinear equation of motion of the meander then takes the form

$$\begin{aligned} \frac{\partial\zeta_m}{\partial t} &= -\epsilon a \frac{\partial^2\zeta_m}{\partial x^2} - b \frac{\partial^4\zeta_m}{\partial x^4} \\ &+ c[\zeta_{m+1}(x, t) + \zeta_{m-1}(x, t) - 2\zeta_m(x, t)] \\ &+ d \left(\frac{\partial\zeta_m}{\partial x}\right)^2. \end{aligned} \quad (31)$$

We will check later that d has no ϵ dependence. This equation allows us to determine the scaling of the meander by making the nonlinear term ($\sim \epsilon \zeta^2$) scale like the other terms

($\sim \epsilon^2 \zeta$). We find $\zeta \sim \epsilon$. It follows immediately that the nonlinearities of higher order in ζ (cubic, quartic, etc.) provide higher-order terms.

The full equation (with the linear propagative terms) takes the form [see Eq. (B7)]

$$\begin{aligned} \frac{\partial \zeta_m}{\partial t} = & g_0(\zeta_{m+1} - \zeta_{m-1}) - g_2 \left(\frac{\partial^2 \zeta_{m+1}}{\partial x^2} - \frac{\partial^2 \zeta_{m-1}}{\partial x^2} \right) \\ & + c[\zeta_{m+1}(x,t) + \zeta_{m-1}(x,t) - 2\zeta_m(x,t)] \\ & - \epsilon a \frac{\partial^2 \zeta_m}{\partial x^2} - b \frac{\partial^4 \zeta_m}{\partial x^4} + d \left(\frac{\partial \zeta_m}{\partial x} \right)^2. \end{aligned} \quad (32)$$

The expression of the coefficients is given in Appendix B.

IV. MAIN STEPS IN THE CALCULATION

We use the quasistatic approximation (see the preceding paper). First, we look for a stationary concentration u for a given configuration of the steps. Then, we determine the step velocity from the mass conservation at the steps. In this approximation, the meander dynamics is local in time. We then perform a local spatial expansion of all the quantities involved in the integro-differential system of equations provided by the Green's functions formalism (B5). The derivatives with respect to x with an order higher than 4 are not relevant because $(\partial^{4+n} \zeta / \partial x^{4+n}) \sim \epsilon^{3+n/2} \ll \epsilon^3$, which is the order of the terms of Eq. (31). The concentration u is expanded as a function of the meander

$$\begin{aligned} u_+ = & u_{0+} + \sum_{n=0}^4 \left(\alpha_n + \frac{\partial^n \zeta}{\partial x^n} + \beta_n + \frac{\partial^n \zeta_+}{\partial x^n} \right) \\ & + \sum_{n=1}^{10} \gamma_n \chi_n + \zeta \frac{\partial u_{0+}}{\partial z} + \chi_1 \frac{\partial^2 u_{0+}}{\partial z^2}. \end{aligned} \quad (33)$$

u_0 is the concentration when $\zeta = \zeta_+ = 0$. χ_n are the relevant quadratic nonlinearities (see Appendix B). u_- is expanded in a similar way.

The Green's functions formalism provides integro-differential equations including not only quantities (such as u or ζ) at given x and t , but also an integral contribution of these quantities over space and time. Let x' and t' denote the integration variables. The quasistatic approximation implies that in the kernel of the integral equation both u' and ζ' depend on t and not on t' . More precisely, $u' \equiv u(\mathbf{r}', t') \simeq u(\mathbf{r}', t)$ (with a similar relation for the step position). Consequently, the dependence on t' appears only in the Green's function. We define $\Delta x = x - x'$. We then perform a local expansion of the meander

$$\begin{aligned} \zeta(x', t') = & \sum_{n=0}^4 \frac{\partial^n \zeta}{\partial x^n} \frac{(-\Delta x)^n}{n!}, \\ \zeta_+(x', t') = & \sum_{n=0}^4 \frac{\partial^n \zeta_+}{\partial x^n} \frac{(-\Delta x)^n}{n!}. \end{aligned} \quad (34)$$

The concentration $u' = u(x', t)$ is then expanded with the help of these relations

$$\begin{aligned} u'_+ = & u_{0+} + \sum_{n,m}^{n+m \leq 4} \left(\alpha_n + \frac{\partial^{n+m} \zeta}{\partial x^{n+m}} + \beta_n + \frac{\partial^{n+m} \zeta_+}{\partial x^{n+m}} \right) \frac{(\Delta x)^m}{m!} \\ & + \sum_{n=1}^{10} \gamma_n \chi_n - \Delta x \sum_{n=4}^{10} \tilde{\gamma}_n \chi_n + (\Delta x)^2 \sum_{n=8}^{10} \gamma_{n-7} \chi_n \\ & + \frac{\partial u_{0+}}{\partial z} \sum_{n=0}^4 \frac{(-\Delta x)^n}{n!} \frac{\partial^n \zeta}{\partial x^n} \\ & + \chi_1 \frac{\partial^2 u_{0+}}{\partial z^2} - \Delta x \chi_4 \frac{\partial^2 u_{0+}}{\partial z^2} + (\Delta x)^2 \chi_8 \frac{\partial^2 u_{0+}}{\partial z^2}, \end{aligned} \quad (35)$$

where $\tilde{\gamma}_4 = \gamma_1$, $\tilde{\gamma}_5 = \gamma_2$, $\tilde{\gamma}_6 = \gamma_2$, $\tilde{\gamma}_7 = \gamma_3$, $\tilde{\gamma}_8 = \gamma_4$, $\tilde{\gamma}_9 = \gamma_5 + \gamma_6$, and $\tilde{\gamma}_{10} = \gamma_7$. The concentration u'_- , together with the Green's function, is expanded in a similar way. Then the integration over x' and t' is performed. The result is formally written in a truncated Taylor expansion of an expression involving the two functions ζ and ζ_+ :

$$\begin{aligned} 0 = & \sum_{n=0}^4 \left(F_n \frac{\partial^n \zeta}{\partial x^n}(x,t) + F_{n+} \frac{\partial^n \zeta_+}{\partial x^n}(x,t) \right) \\ & + \sum_{n=1}^{10} F_{\chi_n} \chi_n(x,t), \end{aligned} \quad (36)$$

where the coefficients F_n , F_{n+} , and F_{χ_n} are known quantities. Since ζ_+ and ζ_- are small but arbitrary functions at this stage, we must have $F_n = 0$, $F_{n+} = 0$, and $F_{\chi_n} = 0$. This relations leads to a linear system of equations for the parameters α_n , β_n , and γ_n . We finally solve this linear system and find the expressions of α_n , β_n , and γ_n . The next step consists in calculating the step velocity from the mass conservation at the steps

$$\frac{V + \zeta}{\left[1 + \left(\frac{\partial \zeta_m}{\partial x} \right)^2 \right]^{1/2}} = D \left(\frac{\partial u_{m,+}}{\partial n} - \frac{\partial u_{m-1,-}}{\partial n} \right). \quad (37)$$

The normal derivatives $\partial u / \partial n$ are evaluated with the help of the deterministic part of the relation (24) of the preceding paper. We can check that the linear part gives the same result as that obtained from a local expansion ($k \rightarrow 0$) of the susceptibility, which is given by Eq. (B15) of the preceding paper. The resulting nonlinear evolution equation of the meander is given by Eq. (32).

V. NONLINEAR STEPS DYNAMICS

The dynamics of a train of steps obeying Eq. (32) is studied numerically in this section. We consider the case where the supersaturation is large enough (above the threshold), so that the noise term is irrelevant (see Sec. II D). We first normalize the deterministic part of Eq. (32) to reduce the description to a minimum number of independent parameters. We define the variables X , T , and ξ as

$$x = \epsilon^{\partial_x} g_x^{-1} X, \quad t = \epsilon^{\partial_t} g_t^{-1} T, \quad \zeta = \epsilon^{\partial_\zeta} g_\zeta \xi. \quad (38)$$

The normalization constants are defined in Appendix B. The evolution equation of a train of steps then reduces to a three-parameter equation

$$\begin{aligned} \frac{\partial \xi_m}{\partial T} = & \left(\eta_0 - \eta_2 \frac{\partial^2}{\partial X^2} \right) \frac{1}{\epsilon} (\xi_{m+1} - \xi_{m-1}) \\ & + \alpha \frac{1}{\epsilon^2} (\xi_{m+1} + \xi_{m-1} - 2\xi_m) \\ & - \frac{\partial^2 \xi_m}{\partial X^2} - \frac{\partial^4 \xi_m}{\partial X^4} + \left(\frac{\partial \xi_m}{\partial X} \right)^2. \end{aligned} \quad (39)$$

The numerical study of this equation is performed with a train of 11 steps using 1024 mesh points. The lateral size of the surface is $L = 2\pi/0.007 \approx 900$. We have used periodic boundary conditions in both directions. The duration of a simulation is $t = (1024 \times 10^2) \times (2 \times 10^{-2})$. The spectra are averaged over eight simulations. We evaluate two quantities: the static spectrum of a step

$$\langle |\xi_k|^2 \rangle = \int \int \frac{d\omega d\omega'}{(2\pi)^2} \int \int \frac{d\Phi d\Phi'}{(2\pi)^2} \int \frac{dk'}{2\pi} \langle \xi_{\omega k \Phi} \xi_{\omega' k' \Phi'} \rangle \quad (40)$$

and the temporal spectrum

$$\begin{aligned} \langle |\xi_\omega|^2 \rangle &= \int \int \frac{dk dk'}{(2\pi)^2} \int \int \frac{d\Phi d\Phi'}{(2\pi)^2} \int \frac{d\omega'}{2\pi} \langle \xi_{\omega k \Phi} \xi_{\omega' k' \Phi'} \rangle. \end{aligned} \quad (41)$$

In this preliminary version, it must be understood that longer simulations are necessary if one wants to extract characteristic exponents. This will be the task of a future work. Here the simulation is only indicative of the detection of special frequencies.

We first study the case of weak propagative effects. We therefore take $\alpha = 1$ and $\eta_0 = \eta_2 = 0.1$. The dynamics is found to be spatiotemporally chaotic. The steps evolve rapidly into the in-phase mode. The static spectrum of a step is identical to that for an isolated step governed by the Kuramoto-Sivashinsky equation (see Fig. 4). In particular, for small wave vectors, $\langle |\xi_k|^2 \rangle \sim k^{-2}$. There is a bump centered on the most unstable wave vector $k = 1/\sqrt{2}$. The temporal spectrum has no characteristic frequency. This means that the meander is strictly temporally chaotic (see Fig. 5).

To study the opposite situation where propagative effects are important, we use another set of parameters: $\alpha = 1$ and $\eta_0 = \eta_2 = 4$. The static spectrum (Fig. 6) is still similar to the one of the previous case. However, the temporal spectrum is different (Fig. 7). There appears a characteristic frequency ω_0 (we can observe the next harmonic as well). Away from these frequencies the spectrum is similar to the previous one. This means that we have temporal chaos at low frequencies.

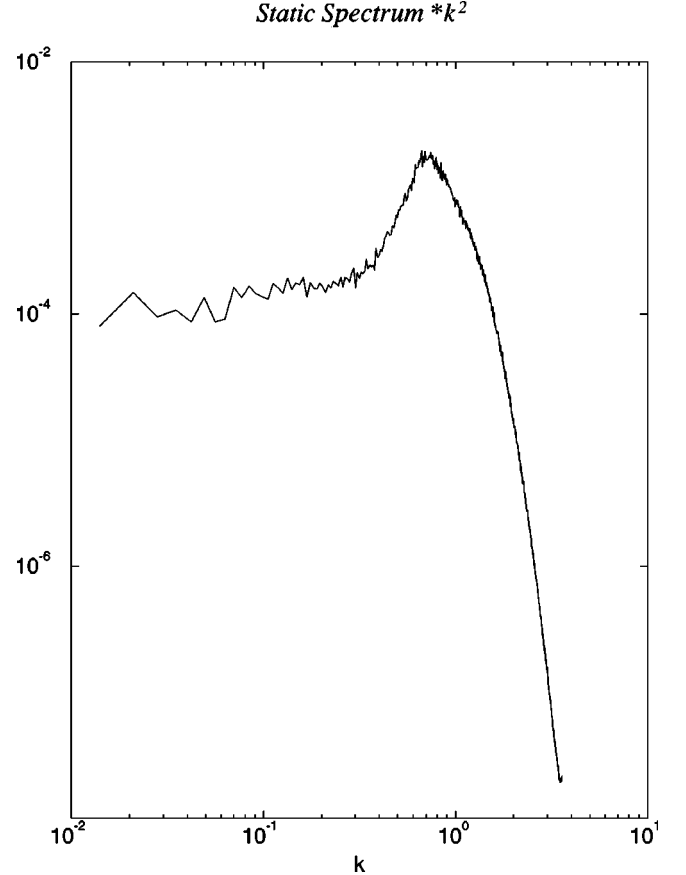


FIG. 4. Static spectrum of the meander as a function of the wave vector. $\alpha = 1$ and $\eta_0 = \eta_2 = 0.1$. The static spectrum is multiplied by k^2 , so that we can easily identify the k^{-2} behavior at small k . We recall that the most unstable mode has a wave vector $k = 2^{-1/2}$.

The short time behavior is a consequence of the propagative effects. The perturbations are advected backward with the velocity $v_0 = -l\omega_0$.

VI. CONTINUUM THEORY

In the previous sections the step was considered as an entity. This section aims at describing the surface evolution at large scales, starting from steps dynamics where the step notion loses its meaning. We consider for that purpose that the steps are separated by a distance that is small in comparison to the characteristic length scale, namely, the diffusion length. More generally, this study focuses on scales that are large in comparison to the interstep distance. We hence define the function $\zeta(y, x, t)$ of the continuum variable y as $\zeta(y = ma_0, x, t) = \zeta_m(x, t)$, where a_0 is the atomic height. The finite difference expressions with respect to m are interpreted as differentiation with respect to y in a Taylor expansion. For example,

$$\zeta_{m+1} - \zeta_{m-1} = 2a_0 \frac{\partial \zeta}{\partial y} + \frac{a_0^3}{3} \frac{\partial^3 \zeta}{\partial y^3} + \mathcal{L}. \quad (42)$$

Since the phase Φ in the Fourier space scales like ϵ , this expression implies that $y \sim \epsilon^{-1}$. The second term on the

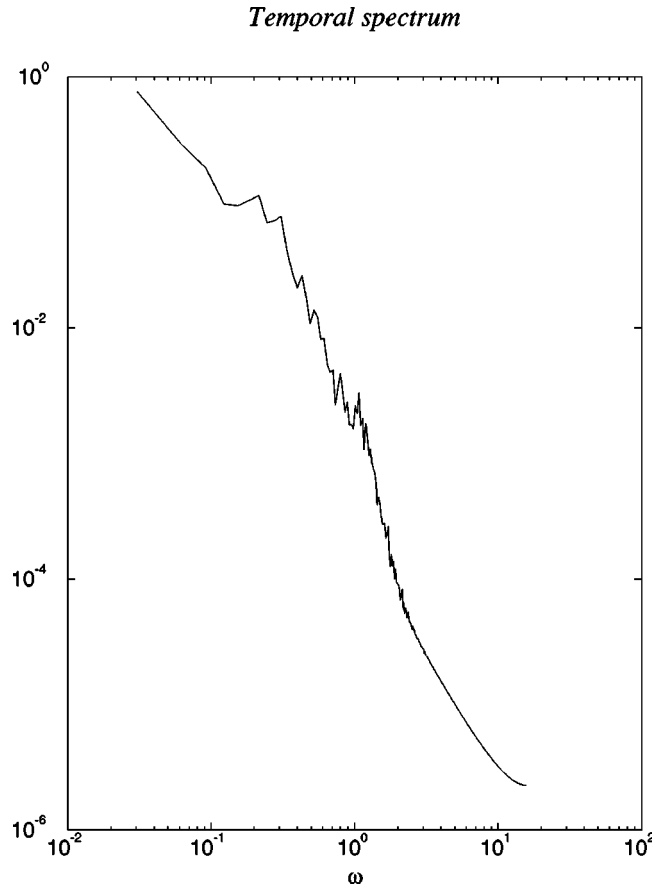


FIG. 5. Temporal spectrum integrated over k and Φ . $\alpha=1$ and $\eta_0=\eta_2=0.1$. There is no characteristic frequency.

right-hand side of Eq. (42) indicates that the first correction is $\sim \epsilon^3$. The evolution equation of the train (B7) is now written as

$$\begin{aligned} \frac{\partial \zeta}{\partial t} = & 2a_0 \left(g_0 - g_2 \frac{\partial^2}{\partial x^2} \right) \frac{\partial \zeta}{\partial y} + ca_0^2 \frac{\partial^2 \zeta}{\partial y^2} \\ & - a \frac{\partial^2 \zeta}{\partial x^2} - b \frac{\partial^4 \zeta}{\partial x^4} + d \left(\frac{\partial \zeta}{\partial x} \right)^2. \end{aligned} \quad (43)$$

We now look for the evolution equation of the surface height. Following the notations of Fig. 8, we define two equivalent representations of the position of the surface

$$\mathcal{Z}(y,x,t) = -\frac{l}{a_0}y + \zeta(y,t), \quad (44)$$

$$\mathcal{Y}(z,x,t) = -\frac{a_0}{l}z + v(z,t).$$

For convenience, we will omit the time dependence of ζ and v in the following. A geometrical relation follows immediately from Eq. (44),

$$v(z) = \frac{a_0}{l} \zeta \left(-\frac{a_0}{l}z + v(z) \right), \quad (45)$$

whose first-order expansion in ζ reads

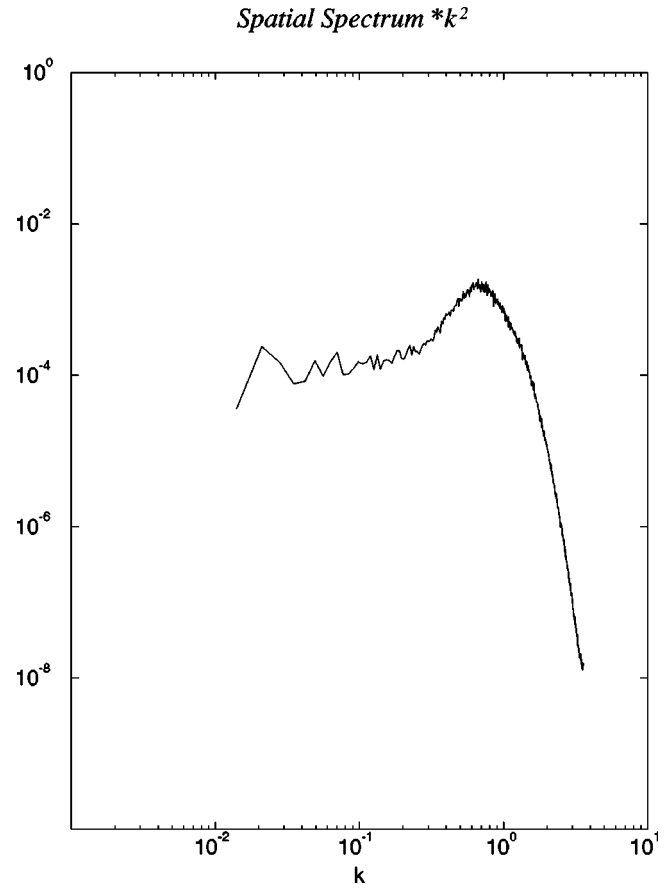


FIG. 6. Static spectrum of the meander. $\alpha=1$ and $\eta_0=\eta_2=4$. The static spectrum is similar to the one obtained in the case of weak propagative effects, where $\eta_0=\eta_2=0.1$.

$$\begin{aligned} v(z) = & \frac{a_0}{l} \zeta \left(-\frac{a_0}{l}z \right) \\ & + \frac{a_0^2}{l^2} \zeta \left(-\frac{a_0}{l}z \right) \frac{\partial \zeta}{\partial y} \left(-\frac{a_0}{l}z \right) + \mathcal{H}. \end{aligned} \quad (46)$$

Since $\zeta \sim \epsilon$, we also have $v \sim \epsilon$. Furthermore, the first correction in Eq. (46) is of order ϵ^3 (i.e., two orders smaller than the first term). Moreover, the derivatives of v with respect to z are

$$\frac{\partial v}{\partial z} = -\frac{a_0^2}{l^2} \frac{\partial \zeta}{\partial y} \left(-\frac{a_0}{l}z \right) + \mathcal{H}, \quad (47)$$

$$\frac{\partial^2 v}{\partial z^2} = \frac{a_0^3}{l^3} \frac{\partial^2 \zeta}{\partial y^2} \left(-\frac{a_0}{l}z \right) + \mathcal{H}.$$

Using Eq. (43), we are now able to write the evolution equation of the surface

$$\begin{aligned} \frac{\partial v}{\partial t} = & \frac{2}{l} \left(-g_0 + g_2 \frac{\partial^2}{\partial x^2} \right) \frac{\partial v}{\partial z} \\ & + \frac{c}{l^2} \frac{\partial^2 v}{\partial z^2} - \epsilon a \frac{\partial^2 v}{\partial x^2} - b \frac{\partial^4 v}{\partial x^4} + d \frac{l}{a_0} \left(\frac{\partial v}{\partial x} \right)^2. \end{aligned} \quad (48)$$

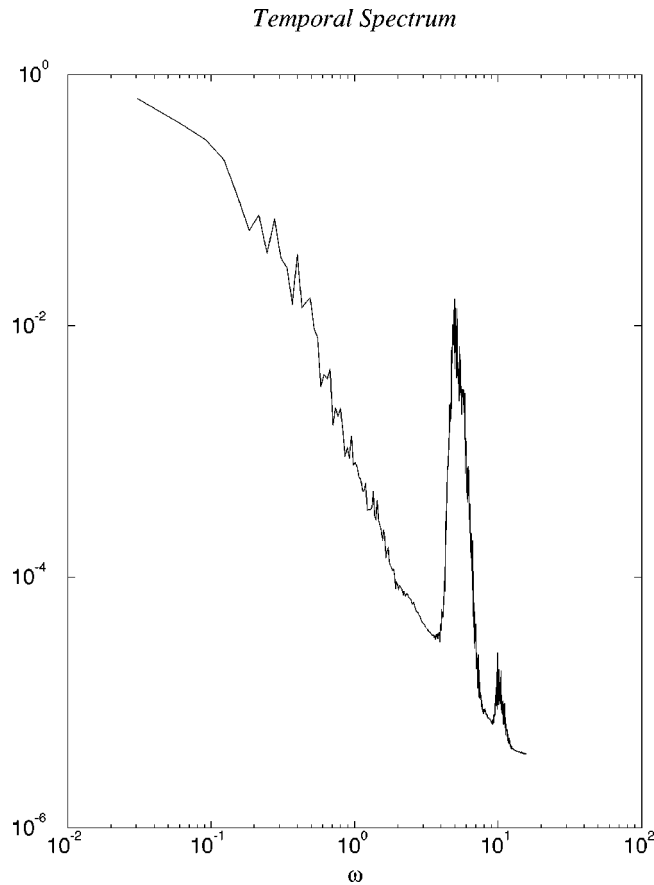


FIG. 7. Temporal spectrum. $\alpha=1$ and $\eta_0 = \eta_2=4$. There is a characteristic pulsation for $\omega \approx 5$ and another for $\omega \approx 10$.

To simplify the numerical investigations and obtain the physical pertinent parameters of this equation, it is useful to normalize space, time, and the amplitude of the perturbation v . The propagative term proportional to g_0 can be absorbed in the time derivative by means of a Galilean transformation $x \rightarrow x + g_0 t$. We obtain a one-parameter equation

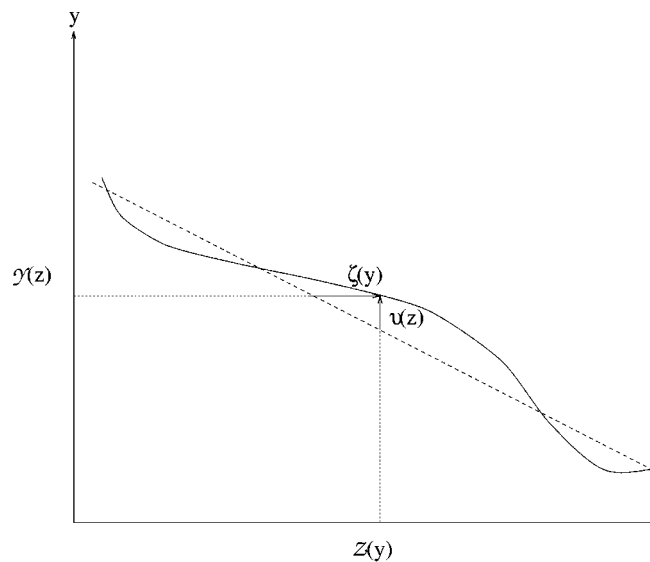


FIG. 8. In the continuum limit two representations are possible: $Z(y, x, t)$ or $Y(z, x, t)$.

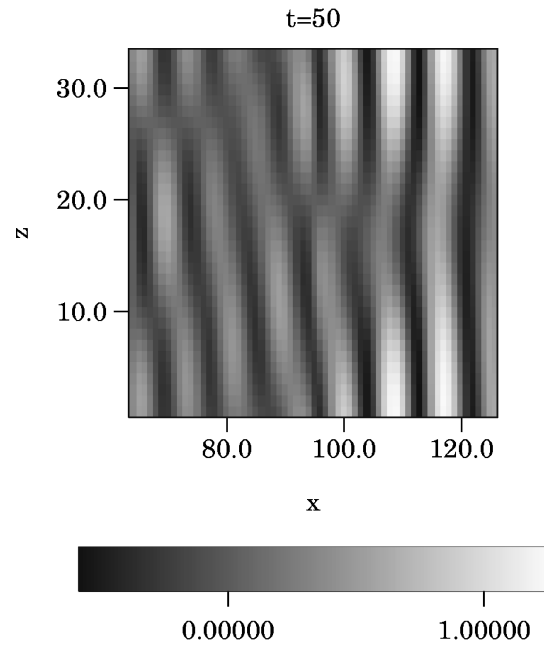


FIG. 9. Initial stage at $t = 50$ and with $\tilde{\eta}_2 = 0$. Stripes take place.

$$\frac{\partial Y}{\partial t} = \tilde{\eta}_2 \frac{\partial^3 Y}{\partial Z X^2} + \frac{\partial^2 Y}{\partial Z^2} - \frac{\partial^2 Y}{\partial X^2} - \frac{\partial^4 Y}{\partial X^4} + \left(\frac{\partial Y}{\partial X} \right)^2, \quad (49)$$

where the variables X and T are normalized according to Eq. (38), $Y = \epsilon^{\theta \epsilon} (a_0/l) g_\epsilon v$, and $Z = \epsilon^{-1} [(bc)^{1/2}/al] z$. We have introduced the notation $\tilde{\eta}_2 = 2\beta_2/\sqrt{\alpha}$.

This equation has been studied by Rost and Krug⁹ in the absence of the propagative term (the term proportional to $\tilde{\eta}_2$). Their result indicates that a chaotic pattern should arise. However, it has been shown elsewhere¹⁰ that the presence of propagative terms could cause drastic changes in the morphology of the surface. We therefore perform a numerical study of the full equation.

Deterministic surface roughening

We shall restrict ourselves to a brief summary. The deterministic part of Eq. (49) is studied numerically in this section. The simulations are done on a 64-unit lattice with periodic boundary conditions. We present the results obtained for two different values of $\tilde{\eta}_2$, with random initial conditions.

In the first case there is no propagative term $\tilde{\eta}_2 = 0$. We see first the primary instability of the meander. Ripples form on the surface (Fig. 9; $t = 50$). This morphology is then destabilized (see Fig. 10; $t = 10^4$).

In the second case there is a strong propagative term $\tilde{\eta}_2 = 5$. There is also the same primary instability as in the previous case (Fig. 11). The surface is destabilized on shorter time scales. The resulting morphology is chaotic. The pattern has lost the $z \rightarrow -z$ symmetry (Fig. 12). The whole pattern is advected in the z direction. We plan to report extensive studies elsewhere.

VII. CONCLUSION

In this and the preceding paper we have given a general description of vicinal surfaces dynamics. In the first paper we

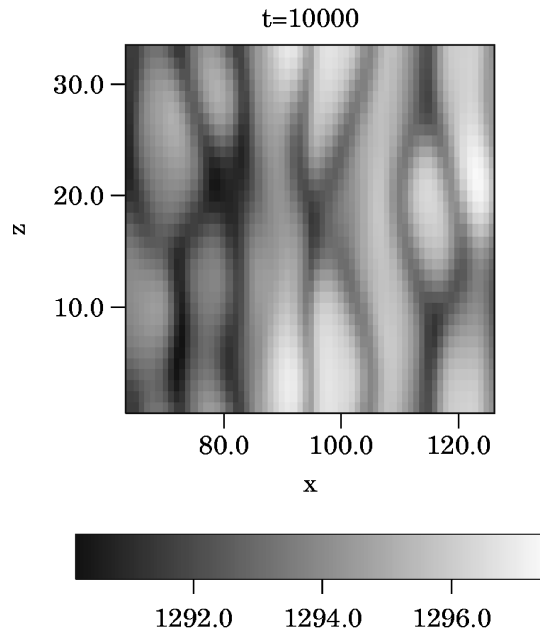


FIG. 10. At a larger time ($t=10^4$) and with $\tilde{\eta}_2=0$ the initial pattern is destabilized.

dealt with the presentation of the full model including an appropriate Langevin formalism. The linear theory was then presented. Several different features were revealed. Among them is the behavior of the out-of-equilibrium roughness. Elastic repulsions are overcome by diffusive repulsion, thereby leading to a drastic reduction of the step meander. This should be the first noticeable feature manifested out of equilibrium. On increasing the incoming flux, the steps become morphologically unstable. We have given a transparent criterion for the instability. The dimensionless critical supersaturation is given by the ratio of a capillary length ($\Omega\Gamma/k_B T$) over the smallest length (the diffusion length, the

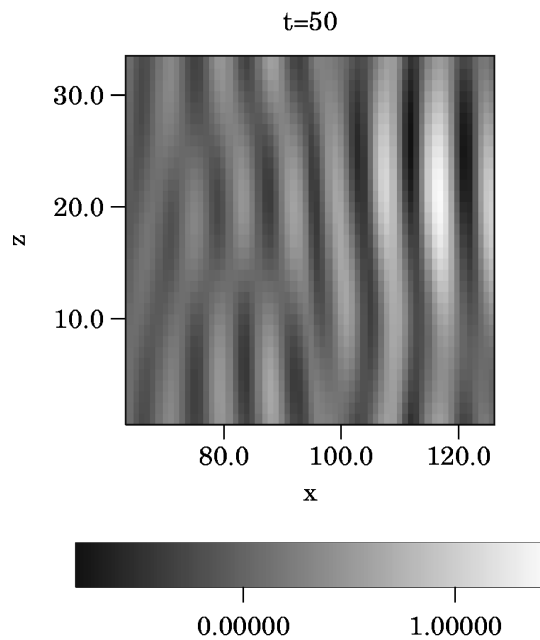


FIG. 11. Primary instability of the vicinal surface. $t=50$ and $\tilde{\eta}_2=5$. There is no difference from the case $\tilde{\eta}_2=0$.

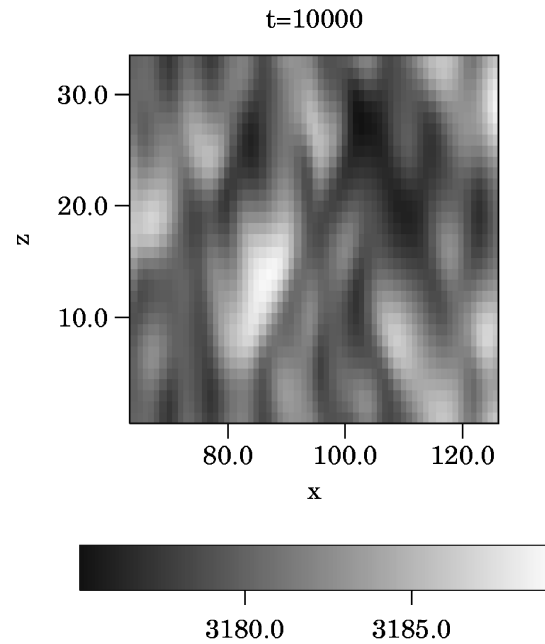


FIG. 12. $t=10^4$ and $\tilde{\eta}_2=5$. The pattern is chaotic. The surface has lost the symmetry $z \rightarrow -z$.

interstep distance, or the Erlich-Schwöebel length). Close to this threshold the roughness diverges (a natural consequence of the instability). In a train of steps this divergence behaves as $\epsilon^{-1/4}$ and not as $\epsilon^{-1/2}$ as is the case for an isolated step (ϵ is the distance from the threshold). Close to the threshold nonlinear terms become important. This paper has been devoted to this situation. We have concentrated on the situation close to the instability threshold. This has the advantage of extracting from a multiscale analysis the relevant nonlinearities. We have shown, on the proviso that desorption is not negligibly small (see below), that the first nonlinearity falls in the KPZ class. While this nonlinearity is usually introduced phenomenologically, here we derive it from physical first principles. Moreover, this allows us to determine its amplitude as a function of thermodynamic and transport coefficients. Each step is governed by a partial differential equation, coupled to its neighbors, through both the adatom diffusion and the elastic field. The relevant nonlinearity is of KPZ or Kuramoto-Sivashinsky (KS) type. The equation contains in addition propagative terms leading to advection in the direction opposite the train motion. The propagative character is due to coupling to other steps and to the breakdown of the mirror symmetry along the vicinal direction.

We have analyzed the case of an isolated step. In that limit the equation is of KPZ or noisy-KS type (depending on whether the incoming flux is below or above its critical value). We have pointed out the strong competition between stochastic effects (thermal noise that is strong due the inherent one-dimensional character of the steps) and deterministic effects (produced by spatiotemporal chaos). By using simple scaling arguments we have determined the region around the critical supersaturation where stochasticity and determinism compete. Outside this region the dynamics is of either KPZ (below threshold) or KS (above threshold) type.

In a train of steps new coupling terms appear, which are either of diffusive or propagative nature. In order to make

contact with traditional surface phenomenological equations, we have determined from step equations the evolution equation for the surface starting from individual step descriptions. Close to the threshold the equation is of anisotropic Kuramoto-Sivashinsky type, containing propagative terms [Eq. (49)]. This equation differs from those used phenomenologically in the literature by the presence of propagative terms.^{9,11} It will thus be an important task for future investigation to elucidate their effects in the study of kinetic roughening of a vicinal surface, such as that studied by Wolf.¹¹

The continuum version [Eq. (49)] of our step equations has been analyzed numerically. At small times the surface develops ripples that are elongated along the step motion. This is the consequence of the step morphological instability. As time elapses, the ripples undergo a zigzag instability (secondary instability), an instability leading ultimately to a rough surface. The morphology is very reminiscent of that obtained when 2D nucleation is present. This morphology also bears resemblance to that obtained by Rost *et al.*,³ in which desorption was ignored.

There are several future lines of investigations. First, our equations can now be fully integrated without resorting to the near-threshold limit. We hope to report along these lines in the future. In the nonlinear study we have limited ourselves to the situation where desorption was not negligible on all scales of interest. We have assumed that the wavelength of the pattern is large in comparison to all other lengths and in particular larger than the diffusion length. If this does not hold, a full study is necessary. This is the regime where many growth experiments are performed. From the analytical point of view, it turns out that the no-desorption limit is singular in the sense that the amplitude does not scale down to zero at the instability limit.¹² In this work we have not taken into account 2D nucleation. This phenomenon would constitute a step in the approaching dynamics of a nominal high symmetry surface, a regime that has induced recently several investigations.¹³

ACKNOWLEDGMENTS

We are grateful to T. Ihle, A. Karma, J. Krug, P. Nozières, A. Pimpinelli, and J. Villain for many enlightening discussions. We are grateful to the Centre Grenoblois de Calcul Vectoriel for providing us with computing facilities. Part of the work of O.P.L. was supported by NSF-sponsored MRSEC, Grant No. DMR 96-32521.

APPENDIX A: LINEAR ANALYSIS FOR AN ISOLATED STEP

To first order in ζ , Eq. (4) reads

$$0 = \frac{\Gamma}{2} \frac{\partial^2 \zeta}{\partial x^2} + \frac{\Omega}{2} \eta_+ + \int dt' \int dx' \frac{Y(\Delta t)}{4\pi D \Delta t} \times e^{-\Delta t/\tau - (\Delta x)^2/4D\Delta t} \times \left\{ \frac{1}{2\Delta t} \left(-\frac{\partial \zeta'}{\partial x} \Delta x + \Delta \zeta \right) [-\Omega c_{eq}^0 \sigma] \right.$$

$$\left. -\zeta' - \Omega q'_z + \zeta' \Omega c_{eq}^0 \sigma \right\} + \Omega \int dt' \int dx' \int dz' \frac{Y(\Delta t)}{4\pi D \Delta t} \times e^{-\Delta t/\tau - [\Delta x^2 + (z' - \zeta)^2]/4D\Delta t} \{f' - \nabla \cdot \mathbf{q}'\}. \quad (\text{A1})$$

In Fourier space, Eq. (A1) is easily integrated, using the relations for the deterministic part, with $\zeta = e^{-i(\omega\Delta t + k\Delta x)} \zeta_{\omega k}$,

$$\int dt' \int dx' \frac{Y(\Delta t)}{4\pi D \Delta t} e^{-\Delta t/\tau - (\Delta x)^2/4D\Delta t} \times \frac{1}{2\Delta t} \left(-\frac{\partial \zeta'}{\partial x} \Delta x + \Delta \zeta \right) = \frac{\zeta_{\omega k}}{2x_s} \left(-1 + x_s \Lambda_{\omega k} - \frac{x_s k^2}{\Lambda_{\omega k}} \right), \quad (\text{A2})$$

$$\int dt' \int dx' \frac{Y(\Delta t)}{4\pi D \Delta t} e^{-\Delta t/\tau - (\Delta x)^2/4D\Delta t} e^{-i(\omega\Delta t + k\Delta x)} = \frac{1}{2x_s \Lambda_{\omega k}}, \quad (\text{A3})$$

where $\Lambda_{\omega k} = (k^2 + i\omega/D + 1/D\tau)^{1/2}$. The resulting equation is given by Eq. (7).

APPENDIX B: MULTIPLE SCALE ANALYSIS

We here perform a multiple scale analysis, where we determine the prefactors of Eq. (31). We will therefore only consider the deterministic part of the equations. In Sec. III B we have shown that the nonlinearity of this equation is $(\partial\zeta/\partial x)^2$. We therefore have to take into account all the nonlinearities whose derivatives can lead to this term. We will first look for the nonlinearities that appear in the normalized concentration u_{\pm} between the steps m and $m+1$. It has been shown in Sec. III B that the terms coming from the elastic repulsion do not provide relevant nonlinearities. We will therefore not consider them. The concentration on a terrace therefore depends only on the position of the steps that surround it. To simplify the expressions, we use the notation $\zeta = \zeta_m$ and $\zeta_+ = \zeta_{m+1}$. We define

$$\chi_1 = \frac{1}{2} \zeta^2, \quad \chi_2 = \zeta \zeta_+, \quad \chi_3 = \frac{1}{2} \zeta_+^2, \quad \chi_4 = \zeta \frac{\partial \zeta}{\partial x},$$

$$\chi_5 = \zeta \frac{\partial \zeta_+}{\partial x}, \quad \chi_6 = \zeta_+ \frac{\partial \zeta}{\partial x}, \quad \chi_7 = \zeta_+ \frac{\partial \zeta_+}{\partial x}, \quad (\text{B1})$$

$$\chi_8 = \left(\frac{\partial \zeta}{\partial x} \right)^2, \quad \chi_9 = 2 \frac{\partial \zeta}{\partial x} \frac{\partial \zeta_+}{\partial x}, \quad \chi_{10} = \left(\frac{\partial \zeta_+}{\partial x} \right)^2.$$

The starting equations to be developed are (see the preceding paper, Appendix B)

$$\begin{aligned}
-\frac{1}{2}u_+ &= \int_0^\infty d\Delta t \left\{ \tau \int_{-\infty}^{+\infty} dx \zeta' u'_+ G(\Delta t, \Delta x, \zeta' - \zeta) \right. \\
&\quad + \tau D \int_{-\infty}^{+\infty} d\Gamma'_s \left(G(\Delta t, \Delta x, \zeta' - \zeta) \frac{\partial u'_+}{\partial n} \right. \\
&\quad \left. \left. - u'_+ \frac{\partial G}{\partial n}(\Delta t, \Delta x, \zeta' - \zeta) \right) \right. \\
&\quad \left. - \tau \int_{-\infty}^{+\infty} dx \zeta'_+ u'_- G(\Delta t, \Delta x, l + \zeta'_+ - \zeta) \right. \\
&\quad - \tau D \int_{-\infty}^{+\infty} d\Gamma'_s \left(G(\Delta t, \Delta x, l + \zeta'_+ - \zeta) \frac{\partial u'_-}{\partial n} \right. \\
&\quad \left. \left. - u'_- \frac{\partial G}{\partial n}(\Delta t, \Delta x, l + \zeta'_+ - \zeta) \right) \right\}, \quad (\text{B2})
\end{aligned}$$

$$\begin{aligned}
&= \left(\frac{\gamma_{8+}}{d_+} + \frac{\gamma_{10-}}{d_-} + \frac{V}{2D} + \frac{\gamma_{10+}}{d_+} \right. \\
&\quad \left. + \frac{\gamma_{8-}}{d_-} + 2\frac{\gamma_{9+}}{d_+} + 2\frac{\gamma_{9-}}{d_-} \right) \left(\frac{\partial \zeta_m}{\partial x} \right)^2 + \dots
\end{aligned} \quad (\text{B4})$$

We finally find an equation of the form

$$\begin{aligned}
\frac{\partial \zeta_m}{\partial t} &= g_0(\zeta_{m+1} - \zeta_{m-1}) - g_2 \left(\frac{\partial^2 \zeta_{m+1}}{\partial x^2} - \frac{\partial^2 \zeta_{m-1}}{\partial x^2} \right) \\
&\quad + c[\zeta_{m+1}(x, t) + \zeta_{m-1}(x, t) - 2\zeta_m(x, t)] - \epsilon a \frac{\partial^2 \zeta_m}{\partial x^2} \\
&\quad - b \frac{\partial^4 \zeta_m}{\partial x^4} + d \left(\frac{\partial \zeta_m}{\partial x} \right)^2, \quad (\text{B5})
\end{aligned}$$

$$\begin{aligned}
-\frac{1}{2}u_- &= \int_0^\infty d\Delta t \left\{ \tau \int_{-\infty}^{+\infty} dx \zeta' u'_+ G(\Delta t, \Delta x, \zeta' - l - \zeta_+) \right. \\
&\quad + \tau D \int_{-\infty}^{+\infty} d\Gamma'_s \left(G(\Delta t, \Delta x, \zeta' - l - \zeta_+) \frac{\partial u'_+}{\partial n} \right. \\
&\quad \left. - u'_+ \frac{\partial G}{\partial n}(\Delta t, \Delta x, \zeta' - l - \zeta_+) \right) \\
&\quad - \tau \int_{-\infty}^{+\infty} dx \zeta'_+ u'_- G(\Delta t, \Delta x, \zeta'_+ - \zeta_+) \\
&\quad - \tau D \int_{-\infty}^{+\infty} d\Gamma'_s \left(G(\Delta t, \Delta x, \zeta'_+ - \zeta_+) \frac{\partial u'_-}{\partial n} \right. \\
&\quad \left. \left. - u'_- \frac{\partial G}{\partial n}(\Delta t, \Delta x, \zeta'_+ - \zeta_+) \right) \right\}, \quad (\text{B3})
\end{aligned}$$

where

$$\begin{aligned}
a &= D \frac{\Gamma}{x_s} \frac{f_0}{D_0}, \\
b &= D \Gamma x_s \frac{C_0}{D_0}, \\
c &= D \frac{1}{x_s D_0} \left[\frac{A}{l^4} f_0 + \frac{\sigma \Omega c_{eq}}{2x_s^3 D_0} (d_-^2 - d_+^2) \right], \\
d &= \frac{V}{2} \left[1 - \frac{l}{x_s} \frac{B_0}{f_0 D_0} \right], \quad (\text{B6})
\end{aligned}$$

where the prime for a function of x and t refers to the arguments x' and t' . The main steps of the calculation are described in Sec. IV. The nonlinear part of the evolution equation reads

$$\begin{aligned}
\left(\frac{1}{D} \frac{\partial \zeta_m}{\partial t} \right)_{\text{nonlin}} &= \left(\frac{\gamma_{8+}}{d_+} + \frac{\gamma_{10-}}{d_-} + \frac{V}{2D} \right) \left(\frac{\partial \zeta_m}{\partial x} \right)^2 \\
&\quad + \frac{\gamma_{10+}}{d_+} \left(\frac{\partial \zeta_{m+1}}{\partial x} \right)^2 + \frac{\gamma_{8-}}{d_-} \left(\frac{\partial \zeta_{m-1}}{\partial x} \right)^2 \\
&\quad + 2\frac{\gamma_{9+}}{d_+} \left(\frac{\partial \zeta_{m+1}}{\partial x} \right) \left(\frac{\partial \zeta_m}{\partial x} \right) \\
&\quad + 2\frac{\gamma_{9-}}{d_-} \left(\frac{\partial \zeta_{m-1}}{\partial x} \right) \left(\frac{\partial \zeta_m}{\partial x} \right)
\end{aligned}$$

$$g_0 = D \sigma \frac{\Omega c_{eq}}{x_s^2} \frac{B_0}{2D_0^2},$$

$$g_2 = D \sigma \Omega c_{eq} \frac{B_0 G_0}{4D_0^3}.$$

The mean step velocity V has the expression

$$V = D \frac{\sigma \Omega c_{eq} f_0}{x_s D_0}. \quad (\text{B7})$$

We have used the notations

$$\mathcal{B}_0 = \frac{1}{x_s^2} \{ (d_+ + d_-)^2 + 2(d_+ + d_-)x_s \sinh(l/x_s) + 2(d_+ d_- + x_s^2) [\cosh(l/x_s) - 1] \},$$

$$\mathcal{C}_0 = \left(\frac{1}{2} \sinh(l/x_s) \left(\frac{d_+ + d_-}{x_s} + \frac{f_0}{\mathcal{D}_0} \right) + \frac{l}{2x_s \mathcal{D}_0} \left\{ \left(\frac{d_+ + d_-}{x_s} \right)^2 - 2 \left[\frac{d_+ + d_-}{x_s} \sinh(l/x_s) + \left(1 + \frac{d_+ d_-}{x_s^2} \right) [\cosh(l/x_s) - 1] \right] \right\} \right)$$

$$+ \frac{\sigma}{\sigma_{BZ}} \frac{1}{4 \sinh(l/x_s)} \left\{ \frac{d_+ + d_-}{x_s} \left(\frac{l^2}{x_s^2} - \sinh^2(l/x_s) \right) + 2 \sinh(l/x_s) \frac{f_0}{\mathcal{D}_0} \left(\frac{d_+ + d_-}{x_s} \cosh(l/x_s) + \frac{d_+ d_-}{x_s^2} \sinh(l/x_s) \right) \right.$$

$$\left. - 2 \frac{l(d_+ + d_-)}{x_s^2} \frac{f_0}{\mathcal{D}_0} \right\}, \quad (\text{B8})$$

$$\mathcal{G}_0 = \left(1 - \frac{d_+ d_-}{x_s^2} \right) \sinh(l/x_s) - \frac{l}{x_s} \left[\frac{d_+ + d_-}{x_s} \sinh(l/x_s) + \left(1 + \frac{d_+ d_-}{x_s^2} \right) \cosh(l/x_s) \right].$$

To recover the case of an isolated step, we take the limit $l \rightarrow \infty$ in Eq. (B7). We find the same result as Eq. (14). We now return to the case of a train of steps. We introduce the normalized variables X , T , and ξ via the relations

$$x = \epsilon^{\partial_x} g_x^{-1} X, \quad t = \epsilon^{\partial_t} g_t^{-1} T, \quad \zeta = \epsilon^{\partial_\zeta} g_\zeta \xi. \quad (\text{B9})$$

The normalization constants are

$$g_x = \frac{1}{x_s} \sqrt{\frac{f_0}{\mathcal{C}_0}}, \quad g_t = \frac{1}{D \tau^2} \Gamma x_s \frac{f_0}{\mathcal{D}_0 \mathcal{C}_0}, \quad g_\zeta = \frac{2\Gamma}{\sigma \Omega c_{eq}} \left(1 - \frac{l}{x_s} \frac{\mathcal{B}_0}{\mathcal{D}_0 f_0} \right)^{-1}. \quad (\text{B10})$$

The three parameters of the resulting equation reads

$$\beta_2 = \sigma \Omega c_{eq} \frac{x_s}{4\Gamma} \frac{\mathcal{B}_0 \mathcal{G}_0}{\mathcal{D}_0^2 f_0}, \quad \beta_0 = \frac{1}{\epsilon} \frac{\mathcal{B}_0 \mathcal{C}_0}{\mathcal{D}_0 f_0^2}, \quad \alpha = \frac{x_s^2}{\Gamma} \frac{\mathcal{C}_0}{f_0} \left[\frac{A}{l^4} + \frac{\sigma \Omega c_{eq} (d_-^2 - d_+^2)}{2x_s^3 \mathcal{D}_0 f_0} \right]. \quad (\text{B11})$$

The evolution equation of the meander now takes the form

$$\frac{\partial \xi_m}{\partial T} = \left(\beta_0 - \beta_2 \frac{\partial^2}{\partial X^2} \right) \frac{1}{\epsilon} (\xi_{m+1} - \xi_{m-1}) + \alpha \frac{1}{\epsilon^2} (\xi_{m+1} + \xi_{m-1} - 2\xi_m) - \frac{\partial^2 \xi_m}{\partial X^2} - \frac{\partial^4 \xi_m}{\partial X^4} + \left(\frac{\partial \xi_m}{\partial X} \right)^2. \quad (\text{B12})$$

*Present address: Physics Department, University of Maryland, College Park, MD 20742-4111.

¹M. Kardar, G. Parisi, and Y.-C. Zhang, Phys. Rev. Lett. **56**, 889 (1986).

²I. Bena, C. Misbah, and A. Valance, Phys. Rev. B **47**, 7408 (1993).

³M. Rost, P. Smilauer, and J. Krug, Surf. Sci. **369**, 393 (1996).

⁴C. Misbah and W.-J. Rappel, Phys. Rev. B **48**, 12 193 (1993).

⁵G. I. Sivashinsky, Annu. Rev. Fluid Mech. **15**, 179 (1983).

⁶C. Misbah, H. Müller-Krumbhaar, and D. E. Temkin, J. Phys. I **1**, 585 (1991).

⁷C. Misbah and A. Valance, Phys. Rev. E **49**, 166 (1994).

⁸A. Karma and C. Misbah, Phys. Rev. Lett. **71**, 3810 (1993).

⁹M. Rost and J. Krug, Phys. Rev. Lett. **75**, 3894 (1995).

¹⁰C. Misbah and O. Pierre-Louis, Phys. Rev. E **53**, R4318 (1996).

¹¹D. E. Wolf, Phys. Rev. Lett. **67**, 1783 (1991).

¹²O. Pierre-Louis, thèse, Université Grenoble I, 1997 (unpublished).

¹³P. Politi and J. Villain, Phys. Rev. B **54**, 5114 (1996).